1964

Water jet air pump theory and performance.

Higgins, Hugh W.

Pennsylvania State University

WATER JET AIR PUMP THEORY AND PERFORMANCE

1964

HUGH W. HIGGINS

The Pennsylvania State University

The Graduate School

Department of Mechanical Engineering

Water Jet Air Pump Theory and Performance

A thesis in

Mechanical Engineering

by

Hugh W. Higgins

Submitted in partial fulfillment
of the requirements
for the degree of

Master of Science

September 1964

ACKNOWLEDGMENTS

The Author wishes to express his appreciation to Dr. R. G. Cunningham who suggested the subject, and under whose guidance this thesis was prepared. The aid of Mr. J. Korman and others in the construction of the apparatus is gratefully acknowledged. The Author also acknowledges the use of the facilities of the Mechanical Engineering Laboratory.

TABLE OF CONTENTS

LIST OF FIGURES

Table of Nomenclature

W = Mass flow rate, lb_m/min

P = static pressure, psf or psi

$\bar{P}$ = total pressure, psf

V = velocity, fps

ρ = density, lb_m/ft^3

A = area, ft^2

D = diameter, ft or in

L = throat length, ft or in

S = nozzle-to-throat spacing, ft or in

g_c = dimensional constant $\frac{lb_m\ ft}{lb_f\ sec^2}$

b = area ratio $\frac{An}{At}$

ϕ = flow ratio $\frac{W_2\ \rho_1}{W_1\ \rho_{2s}} = \frac{Q_{2s}}{Q_1}$

Q = volumetric flow rate, ft^3/min

K_1 = nozzle coefficient

K_3 = throat friction coefficient

K_4 = diffuser friction coefficient

N = dimensionless pressure ratio $\frac{P_d}{P_n - P_d}$

α = dimensionless pressure ratio $\frac{P_d}{P_s}$

η = efficiency = $\phi_d\ N \ln \alpha$

E = power $\frac{ft\ lb_f}{sec}$

SUBSCRIPTS

1 = water

2 = air

m = mixture

m = mean

n = nozzle entry

s = throat entry

t = throat exit, diffuser entry

d = diffuser exit

0 = side flow entry to jet pump

fl = friction loss

ml = mixing loss

c = isothermal gas compression

CHAPTER I

INTRODUCTION

A jet pump is a device that utilizes a momentum transfer action from a high velocity jet fluid to pump another fluid, either the same or different from that of the jet. The liquid jet gas pump is simple in construction, has no moving parts, and is used primarily for pumping gases containing some condensable vapors, such as water vapor, solvent vapors under a vacuum, or others which would be harmful to mechanical pumps.

Statement of the Problem

The jet pump, although in use for many years, has received relatively little attention in the technical literature. The majority of papers have considered either the case of compressible flow such as the analysis by Keenan and Neumann (1)*, or the case of incompressible flow such as the analysis by Gosline and O'Brien (2). Therefore, the objective of this investigation was to develop a theoretical analysis of the liquid-jet gas pump and to evaluate the theory by comparison with experimental results.

Previous Investigations

The water jet air pump has been investigated by Flügel (3), Pawel-Rammengen (4), and others, and some performance data have been reported by Folsom (5). In this latter study Folsom (5) concluded that the performance of the jet pump should be dependent on diffuser characteristics, however in all the studies listed above, no satisfactory analysis of the pumping system was made.

*Numbers in parenthesis refer to the Bibliography.

The most recent study on liquid jet air pumps was reported by Takashima (6), wherein data were obtained for a jet pump in a water circuit using two-inch pipes. The conclusions of this study were based on assumed values for the nozzle discharge coefficient, throat friction factor, and diffuser coefficient.

CHAPTER II

WATER JET-AIR PUMP THEORETICAL ANALYSIS

Derivation and Analysis of Equations

Although the details of the mixing process of the water and air are highly complicated, application of the momentum theory permits a solution by treating the initial stream before mixing, and after mixing has been completed. As shown in Figure 1, the water jet penetrates the slowly moving air, and as mixing occurs momentum transfer accelerates the air in the throat. As the flow of air and water progresses the mixture stream spreads until at the throat exit, it touches the wall of the throat.

The following assumptions are made:

(1) The flow streams are one-dimensional at throat entrance and exit.

(2) Mixing is completed in the constant area throat, against an adverse pressure gradient.

(3) Suction chamber pressure is constant throughout the chamber, that is, the pressure at the nozzle tip is equal to the pressure at the throat entrance.

(4) Isothermal conditions prevail in the throat-diffuser section because of the relative heat capacities of air and water.

(5) Air acts as an ideal gas, that is $\frac{P_2}{\rho_2} = RT_2$, and water is incompressible, ρ = constant.

Equation of Motion for Liquid Gas Mixture

Assuming negligible change in elevation and steady flow conditions, the equation of motion, including a friction loss term, can be written

$$\frac{dP}{\rho} + \frac{V\,dV}{g_c} + f\,\frac{dx}{D}\,\frac{V^2}{2g_c} = 0 \qquad (1)$$

Where: f = friction coefficient

ρ = mixture density defined as

$\rho = \dfrac{W_1 + W_2}{Q_1 + Q_2}$ subscripts 1 and 2 refer to liquid and gas respectively.

Let the volume ratio $\phi = \dfrac{Q_2}{Q_1}$, and neglect the mass of gas W_2 then,

$$\rho = \frac{W_1}{Q_1\,(1 + \phi)} = \frac{\rho_1}{1 + \phi}$$

Let ϕ_s represent Q_{2s}/Q_1, the flow ratio at pump inlet, and assume that the gas phase behaves as a perfect gas under isothermal conditions then,

$$\rho = \frac{\rho_1}{1 + \phi_s\,\frac{P_s}{P}} \qquad (2)$$

Within the isothermal flow tube density is a function of absolute pressure only.

Equation (1) can be integrated from a to b using ρ_m:

$$\frac{P_b - P_a}{\rho} + \frac{V_b^2 - V_a^2}{2g_c} + \int_a^b \frac{f\,V^2 dx}{D 2g_c} = 0 \qquad (3)$$

in which the mean density is defined by

$$\rho_m = \frac{P_b - P_a}{\int_a^b \frac{dP}{\rho}} = \frac{P_b - P_a}{\frac{1}{\rho_1}\int_a^b (1 + \phi_s\,\frac{P_s}{P})\,dP}$$

$$\rho_m = \frac{P_b - P_a}{\frac{1}{\rho_1}\,[P + \phi_s P_s \ln P]_a^b} = \frac{\rho_1 (P_b - P_a)}{P_b - P_a + \phi_s P_s \ln \frac{P_b}{P_a}} \qquad (4)$$

Thus equation (3) becomes:

$$\frac{P_b - P_a}{\rho_l} + \frac{\phi_s P_s}{\rho_l} \ln \frac{P_b}{P_a} + \frac{V_b^2 - V_a^2}{2g_c} + \int_a^b \frac{f V^2}{D 2g_c} dx = 0 \qquad (5)$$

Diffuser Equation

Applying equation (5) to the flow from the throat exit (t) to the diffuser exit (d); and basing the friction loss term on the density and velocity at t:

$$P_d + \frac{\rho_l V_d^2}{2g_c} - P_t = \frac{\rho_l V_t^2}{2g_c} - K_4 \frac{\rho_t V_t^2}{2g_c} - \phi_s P_s \ln \frac{P_d}{P_t} \qquad (6)$$

The friction factor K_4 corresponds to $f\frac{L}{D}$ for flow in a pipe. It is convenient to replace the first two terms with $\bar{P}_d$, a total head expression. Although this is approximate (through use of ρ_l instead of ρ_d) the error is negligible since the kinetic head at the pump discharge (d) is small.

The throat and nozzle velocities are related by continuity:

$$V_t = b\,(1 + \phi_t)\, V_{ls} \qquad (7)$$

Where $b = \frac{A_n}{A_t}$ and $\phi_t = \frac{Q_{2t}}{Q_l} = \phi_s \frac{P_s}{P_t}$ (Isothermal flow)

The diffuser equation can now be rewritten as follows:

$$\bar{P}_d - P_t = \frac{\rho_l V_{ls}^2}{2g_c} \left[b^2(1 + \phi_t)^2 - K_4 b^2 (1 + \phi_t)\right] - \phi_s P_s \ln \frac{P_d}{P_t} \qquad (8)$$

The Throat Equation of Motion.

Equation (5) can be applied between the throat inlet (s) and exit (t). In addition to friction, the throat equation must include a second loss term, E_{ml}, which is required for the irreversible mixing losses that accompany the entrainment of gas by the liquid jet.

$$\frac{P_t - P_s}{\rho_l} + \frac{\phi_s P_s}{\rho_l} \ln \frac{P_t}{P_s} + \frac{V_t^2 - V_{ls}^2}{2g_c} + \int_s^t \frac{fV^2 dx}{D2g_c} + E_{ml} = 0 \qquad (9)$$

For the liquid/liquid jet pump it was shown in reference 7 that the mixing loss is of the form

$$E_{ml} = \frac{V_{ls}^2}{2g_c} [f(b, \phi_w)]$$

where ϕ_w is the mass ratio of secondary liquid to primary liquid stream.

This relation is obtained by writing both the momentum equation and the equation of motion across the jet pump throat, and eliminating the pressure difference term, $P_t - P_s$. It can be shown that the expression reduces to the following form when $\phi_w = 0$, that is, when the secondary liquid flow is zero:

$$E_{ml} = \frac{V_{ls}^2}{2g_c} [1 - 2b + b^2] \qquad (10)$$

This will be recognized as the usual "sudden enlargement loss" for a pipeline, where $b = \frac{A_a}{A_b}$, the ratio of pipe area before and after the enlargement.

Just as the gas phase energy input term at (s) can be neglected due to the small magnitude of W_2 compared to W_1, the useful gain in momentum by the gas phase in the mixing process will be neglected, permitting use of this sudden enlargement loss in equation (9):

$$\frac{P_t - P_s}{\rho_l} + \frac{\phi_s P_s}{\rho_l} \ln \frac{P_t}{P_s} + \frac{V_t^2 - V_{ls}^2}{2g_c} + \int_s^t \frac{fV^2 dx}{D2g_c} + \frac{V_{ls}^2}{2g_c} (1 - 2b + b^2) = 0 \qquad (11)$$

With the friction loss again based on density and velocity at station (t), and using the continuity equation (7), the throat equation (11) becomes:

$$P_t - P_s = \frac{\rho_l V_{ls}^2}{2g_c} [2b - b^2(1 + \phi_t)^2 - b^2 - K_3 b^2 (1 + \phi_t)] - \phi_s P_s \ln \frac{P_t}{P_s} \quad (12)$$

The diffuser and throat equations can be added to obtain:

$$\bar{P}_d - P_s = \frac{\rho_l V_{ls}^2}{2g_c} [2b - b^2 - K_{34} b^2 (1 + \phi_t)] - \phi_s P_s \ln \frac{P_d}{P_s} \quad (13)$$

Where $K_{34} = K_3 + K_4$, for the throat and diffuser.

Nozzle Equation.

The primary or nozzle fluid is of constant density thus:

$$\frac{P_n}{\rho_l} + \frac{V_n^2}{2g_c} = \frac{P_s}{\rho_l} + \frac{V_{ls}^2}{2g_c} + \frac{K_l V_{ls}^2}{2g_c}$$

where the final term represents the friction losses.

Let $\bar{P}_n = P_n + \frac{\rho_l V_n^2}{2g_c}$, the total head, thus

$$\bar{P}_n - P_s = (1 + K_l) \frac{\rho V_{ls}^2}{2g_c} \quad (14)$$

Overall Pressure Drop Equation.

Subtracting equation (13) from equation (14),

$$\bar{P}_n - \bar{P}_d = \frac{\rho_l V_{ls}^2}{2g_c} [1 + K_l - 2b + b^2 + K_{34} b^2 (1 + \phi_t)] + \phi_s P_s \ln \frac{P_d}{P_s} \quad (15)$$

Jet Pump Efficiency.

Assuming isothermal compression of the gas phase in the throat and diffuser, the useful power out is:

$$E_{out} = W_2 \frac{P_d}{\rho_{2d}} \ln \frac{P_d}{P_s}$$

$$E_{in} = W_1 \frac{(\bar{P}_n - \bar{P}_d)}{\rho_l}$$

Since for all practical purposes $P_d = \bar{P}_d$

$$\text{Efficiency } \eta = \frac{W_2}{W_1} \frac{\rho_l}{\rho_{2d}} \quad \frac{P_d \ln \frac{P_d}{P_s}}{\bar{P}_n - \bar{P}_d} \tag{16}$$

$$\eta = \phi_d \frac{\bar{P}_d}{\bar{P}_n - \bar{P}_d} \ln \frac{P_d}{P_s}$$

With N representing the first term and $\alpha = \frac{P_d}{P_s}$,

$$\eta = \phi_d N \ln \alpha \tag{17}$$

Significance of the ln Terms.

The term $\frac{\phi_s P_s}{\rho_l} \ln \frac{P_b}{P_a}$ appears in the equation of motion when the mixture density varies isothermally. This represents work (ft lb_f/lb_m liquid) by the liquid on the gas phase and as such is an energy loss to the liquid phase. Note that the term subtracts from the pressure difference just as the friction loss term does.

Viewed from the gas phase, an observer moving with a gas bubble would see the bubble change in diameter, and the work performed would be:

$$W = \int_a^b P \, d\frac{1}{\rho} = \frac{P}{\rho} \ln \frac{P_b}{P_a} \frac{\text{ft lbf}}{lb_m \text{ gas}}$$

for isothermal conditions, where ρ is the gas density. The correspondence of this term to the "loss" term in the equation of motion is obvious.

The first law of thermodynamics applied to the isothermally compressed bubble shows that a quantity of heat must be transferred out of the gas, which is equal in magnitude to the work term.

This heat is received by the liquid phase and a temperature rise must result. Because of the relatively large heat capacity of the liquid this temperature rise is negligible. Note that equations of

motion, rather than energy equations (which would include internal energy and heat terms) are adequate and appropriate for this analysis. The isothermal work of compression term, however, stems from the gas-phase energy equation.

It is interesting to note that the expenditure of mechanical enrgy of the liquid as work on gas bubbles, and the necessary return of heat energy to the liquid corresponds in net effect to fluid friction, that is mechanical energy is degraded to heat energy, appearing as a liquid temperature rise.

CHAPTER III

EXPERIMENTAL PROCEDURE AND RESULTS

Apparatus

Water Jet Air Pump

A schematic illustration of the experimental water jet air pump and the auxiliary apparatus is shown in Figure 2. The jet pump used, as shown in Figures 3, 4, and 5, was designed to facilitate investigation of the variable area ratio b, and spacing S, and was patterned after a pump used in a previous work by Cunningham (7). It consists of a one inch pipe tee body, with two interchangeable nozzles and two throat-diffuser sections. Therefore four jet pumps could be assembled in one body. All pumps are identified by three numbers; e.g. No. 141/316/300, the numbers referring to nozzle diameter, throat diameter and nozzle-to-throat spacing in thousandths of an inch.

In addition to the two throat-diffuser sections previously described, another throat diffuser section with throat diameter 0.224 inches was made using transparent lucite in order to observe the flow patterns in the throat and diffuser.

Water was supplied to the nozzle from a 130 gallon tank through a centrifugal pump, a one-inch throttle valve, and a rotameter.

A calibrated bourdon tube pressure gage was used to measure nozzle pressure. Air was taken in the top of the pump through a precision wet test meter, a glass water trap, and a throttling valve. The vacuum in the pump body was measured with a U-tube mercury manometer, also containing a water trap. The pressure at the diffuser outlet was measured with two calibrated bourdon tube pressure gages,

inserted upstream of the back pressure valve. Following the back pressure valve, the water-air mixture was discharged to a weigh tank by a flexible hose.

Water Jet Pump

Before the water jet air pump performance data were taken, the apparatus described above was modified to act as a water jet water pump in order to obtain data to compare with well-established performance data previously published by Gosline and O'Brien (2) and Cunningham (7). This modification consisted of disconnecting the air supply to the pump, and connecting a one-inch water supply line through a throttling valve from the pump to the supply tank as shown in Figure 13.

Experimental Procedure

All of the tests were made at a selected nozzle flow rate, W_1, and suction chamber pressure, P_s. The diffuser discharge pressure P_d was varied from the "cutoff" pressure where the air flow rate Q_2 equals zero to the maximum obtainable, where the back pressure valve was wide open, while maintaining P_n, P_s, W_1 constant, air flow rate Q_2 in ft^3/min was recorded.

The rotameter used to indicate primary flow rate W_1, was calibrated as shown in Figure 6, and served only to show steady-flow conditions during a run since the mass flow rate W_1 was determined by timing the pump discharge into a weigh tank..

The five measured quantities were then recorded and converted to the dimensionless flow and pressure ratios N, α and ϕ_d as will be shown in a later chapter.

Results and Comparison With Theory

An initial check on the apparatus was made by modifying the water jet air pump to function as a water jet water pump as described previously. The data obtained compared satisfactorily with data published by Gosline and O'Brien (2) and Cunningham (7) as shown in Appendix A.

Values for the nozzle and throat-diffuser coefficients, K_1 and K_{34} respectively, were computed from test data taken at a flow ratio approximately 2/3 of the maximum-efficiency flow ratio. These values were found to be $K_1 = .18$, and $K_{34} = .051$. These compare with $K_1 = .10$ and $K_{34} = .30$ which Cunningham found at high Reynolds numbers using oil as the fluid (7).

The apparatus was then converted to function as an air pump and tests made. From these data the dimensionless flow ratio ϕ_d was computed and plotted as a function of the two dimensionless pressure ratios N and α as shown in Figures 7 through 10 for various water flow rates and area ratios. Performance of the theoretical model is shown on these curves as a solid line. Numerical results are listed in the test data section, Appendix E.

The relation between $\bar{P}_n - \bar{P}_d$ or $\bar{P}_d - P_s$ and [V_{1s}, b, K_1, K_{34}, ϕ_s, ϕ_t, ϕ_d,] is of interest as a means of constructing an N ln α vs ϕ_d curve. Favorable comparison with test results would validate the treatment.

Obviously there are too many unknowns to permit direct calculation of K's from the test data. This would be possible only if P_t were known. (Folsom pointed out the need for P_t when considering the possibility of a theory-experimental data comparison.)

The friction coefficients can better be measured with liquid/liquid flow or taken from previous works (Reference 7). Nominal (high Reynolds number) values of $K_1 = 0.1$ and $K_{34} = 0.3$ will be used.

Equation 13 can now be solved directly for ϕ_t and hence P_t, using test data, thus giving one use of the theory. Rearrangement of equation 13 yields:

$$\phi_t = \frac{2}{K_{34}b} - 1 - \frac{1}{K_{34}} - \frac{\phi_s P_s}{K_{34}b^2} \frac{\ln \frac{P_d}{\bar{P}_s}}{\frac{\rho_1 V_{1s}^2}{2g_c}} \frac{\bar{P}_d - \bar{P}_s}{K_{34}b^2 \frac{\rho_1 V_{1s}^2}{2gc}} \qquad (18)$$

Sample Calculation:

Pump Number - 173/224/120

Barometer - 28.57 in Hg

Air Temp - 83.5°F

Water Temp 53°F

$Q_2 = 0.121$ ft^3/min at 14.03 psia

$W_1 = 71$ lb_m/min

$P_n = 99.0$ psig (corrected)

P_s -5.8 in Hg or 11.18 psia

$P_d = 60.0$ psig (corrected) $\cong \bar{P}_d = 74.03$ psia

$$N = \frac{P_d}{\bar{P}_n - P_d} = \frac{74.03}{99.0-60.0} = 1.9$$

$$\alpha = \frac{P_d}{P_s} = \frac{74.03}{11.18} = 6.64$$

$$\phi_d = \frac{W_2 \rho_1}{W_1 \rho_{2d}} = 12.22 \quad \frac{Q_2}{P_d} = 0.02$$

$$\phi_s = \phi_d \frac{P_d}{P_s} = .02 \quad \frac{74.03}{11.18} = 0.132$$

K_{34} = 0.3 (assumed)

$$V = \frac{W}{\rho_A} = \frac{71}{60(62.4)1.631 \times 10^{-4}} = 116 \text{ ft/sec}$$

$$\frac{\rho_1 V_{1s}^2}{2g_c} = \frac{62.4\ (116)^2}{64.4} = 13{,}040 \text{ lb}_f/\text{ft}^2$$

Substituting in Equation 18:

$$\phi_t = \frac{2}{(0.3)\ (0.6)} - 1 - \frac{1}{0.3} - \frac{404}{(0.3)\ (0.36)\ (13040)} - \frac{9050}{(0.3)\ (0.36)\ 13040}$$

$$\phi_t = 0.09$$

$$P_t = \frac{\phi_s P_s}{\phi_t} = \frac{(0.132)\ (11.18)}{0.09} = 16.4 \text{ psia}$$

Thus the theory provides a means of finding the throat pressure for measured performance.

Construction of Theoretical Characteristic Curves

Equation 13 could be used as a means of constructing N $\ln\alpha$ and ϕ_d N $\ln\alpha$ (or efficiency) curves if the throat volume ratio ϕ_t could be eliminated as an independent variable. The measured value of ϕ_t (above) is close to the average value,

$$\phi_{t\ avg} = \frac{\phi_s + \phi_d}{2} = \frac{0.132 + 0.02}{2} = 0.076$$

Suggesting the approximation:

$$\phi_t = \frac{\phi_s + \phi_d}{2} \tag{19}$$

with K_{34} = 0.3 and the above approximation for ϕ_t equation 13 can be solved for ϕ_s:

$$\phi_s \left[\frac{P_s \ln \frac{P_d}{P_s}}{K_{34} b^2 \frac{\rho_1 V_{1s}^2}{2g_c}} + \frac{1}{2}\left(1 + \frac{P_s}{P_d}\right) \right] = \frac{2}{K_{34} b} - 1 - \frac{1}{K_{34}} - \frac{\bar{P}_d - P_s}{K_{34} b^2 \frac{\rho_1 V_{1s}^2}{2g_c}} \tag{20}$$

Sample Calculation:

Find ϕ_s for P_d = 60 psig = 74.03 psia with P_s = 11.18 psia and all other data from the above sample calculation.

$$\phi_s\,[2.17 + 0.575] = 11.1 - 1 - 3.33 - 6.41$$

$$\phi_s = \frac{0.36}{2.75} = 0.131, \qquad \phi_d = 0.131\ \frac{11.18}{74.03} = 0.02$$

Similar calculations for other P_d values result in the following:

Assumed P_d	Theoretical ϕ_s	Theoretical ϕ_d
74.03	0.131	0.02
54.03	1.00	0.207
40.03	1.82	0.51
30.03	2.68	0.996
20.02	3.82	2.13
15.03	5.28	3.93
11.18	6.78	6.78

The theoretical curve construction can be completed by solving equation 20 for $\bar{P}_d - P_s$ at $\phi_s = 0$. Here the right side must equal zero, and this shows that P_d = 77.48 psia, therefore,

$$N \ln \mathcal{L} = \frac{77.48}{113.03 - 77.48} \ln \frac{77.48}{11.18} = 4.22$$

The experimental data points are above the theoretical curve at low flow ratios for area ratio b = 0.2. This was assumed to be due to the failure of the flow to conform with the throat wall which in turn could reduce friction, as was originally suggested by Cunningham (7).

Referring to figures 7 through 10 it can be seen that the actual pump performance coincides with theory up to a certain point, and then falls away rapidly. Figures 7A and 10A are complete characteristic curves for figures 7 and 10 respectively. The point at which this

rapid decline occurs coincides with the point at which mixing no longer occurs in the throat. This is shown in the accompanying flow diagrams. Since the theoretical calculations were based upon complete mixing in the throat, they can not be expected to predict actual performance when jet breaking occurs in the diffuser. It can be seen that when the water jet penetrates the entire throat length and does not merge into a water-air mixture until well into the diffuser section, the mixing loss is magnified resulting in a marked loss of efficiency.

The theoretical calculations were derived in Chapter II assuming that the nozzle tip coincided with the throat entrance, that is the pressure at the nozzle tip was assumed equal to the pressure at the throat entrance. In practice, however, the nozzle tip is withdrawn from the throat a distance S in order to obtain optimum performance, and the behavior of the water jet across this distance S could be thought of as a fluid friction energy loss as described by Cunningham (7). This friction loss was calculated and found to be negligible since it was dependent on the density ratio of air to water.

This comparison between theoretical model and actual performance, coupled with visual observations of the change in mixing patterns has shown that (a) the theoretical approach is valid and (b) maximum efficiency demands that the liquid jet gas pump be designed and/or operated to provide jet break-up before entry into the diffuser.

Approximate Flow Ratio at Maximum Efficiency Point.

McElroy (8) observed that the flow ratio at which maximum efficiency occured coincided as a rule with the state of equal momentum at the jet and at the throat discharge.

ie: $W_t V_t = W_l V_{ls}$

in this case

$$W_1 V_t \cong W_1 V_{1s}$$

$$V_{1s} b\ (1 + \phi_t) = V_{1s}$$

$$\phi_{t)_{mep}} = \frac{1-b}{b}$$

For comparison with the water jet air pump, consider the pump with b = 0.2. The above expression yields $\phi_t = 4$. With the assumption that $\phi_t = (\phi_s + \phi_d)/2$, we find that $\phi_{d_{mep}} = 6.9$. A similar calculation for b = 0.6 results in $\phi_{d_{mep}} = 1.21$. Comparison with Figures 7A and 10A show $\phi_{d_{mep}} = 4.0$ and 1.0 respectively, a fairly good check. Apparently this approximate rule of thumb is useful for a water-jet air pump.

Nozzle Throat Spacing

The experimental jet pump as shown in Figure 3 was designed not only to observe the effect of area ratio b on pump performance, but also to study the effect of nozzle-to-throat spacing, S. The nozzle was held in place in the pump body by a nut and O-ring seal. By loosening the nut the nozzle could be moved in and out to change the spacing while the pump was in operation. Scribe marks were placed on the nozzle sections at 0.1 inch intervals.

The optimum value of S was found by initially setting the spacing at one nozzle diameter, and then setting the operating flow ratio ϕ_d equal to approximately two thirds of the value of that obtained at the maximum efficiency point by adjusting the back pressure P_d. The water flow rate W_1 and the suction port pressure P_s were held constant. Optimum spacing was then found by moving the nozzle section in 0.1 inch steps to obtain maximum air flow Q_2 while still holding W_1, P_n, P_s,

and P_d constant.

The results are listed in Table I below:

TABLE I

OPTIMUM NOZZLE - THROAT SPACING

Nominal Area Ratio b	Pump No.	S Inches	S/d_n
0.2	141/316	>1.92	>13.6
0.3	173/316	>1.92	>11.1
0.4	141/224	0.2 - 0.4	1.42 - 2.84
0.6	173/224	0.65	3.75

The optimum spacing S is listed in addition to the ratio of optimum spacing to nozzle diameter, S/d_n. Where more than one value of S is listed the air flow rate remained essentially constant over the range of S values. In other words spacing had a negligible effect on efficiency is the range indicated.

For the nominal area ratios of 0.2 and 0.3 no optimum is listed since the air flow Q_2 increased with increased spacing up to 1.92 inches, the physical limit of the pump.

The first series of tests for all four area ratios were completed using the spacing S recommended by Cunningham (7) for the liquid-liquid case. The experimental data were then used to plot performance curves as seen in Figures 7 through 10, and the information from these curves was then used to select the flow ratio ϕ_d to calculate the value of optimum spacing.

The S/d_n values listed in Table I show an inconsistancy which is probably due to an interaction with the jet break-up location, that is,

as spacing was increased the jet break-up receded and influenced the efficiency. Pump number 173/224/650 (b = 0.6) is the best guide to optimum spacing since the value of ϕ_d used to determine optimum spacing showed least divergence from theory.

The most important conclusion to be drawn from this section is that pump spacing should be set approximately five times the value of optimum spacing listed for the same pump for the liquid-liquid case.

Observations of the Mixing Process

Observations of the mixing process in the transparent lucite throat-diffuser section indicated that for low back-pressure operation the water jet penetrated the entire length of the throat and part of the diffuser before merging into the water-air mixture. As the back pressure was increased the break-up of the water jet receded until mixing was taking place in the throat as it should be. The flow patterns are shown in Figures 9 and 10.

Comparison of the flow patterns and performance curves leads to the conclusion that optimum performance is obtained when the water jet penetrates most of the throat length, and then the water-air mixture merges to fill the diffuser entrance.

In order to accomplish mixing at the diffuser entrance, section t, it was concluded that either (1) the nozzle tip should be withdrawn to increase S or, (2) the length of the throat should be increased.

The first case was explained earlier in this section, and optimum values of S were found for area ratios b = 0.4 and b = 0.6. The performance of the b = 0.6 pump for optimum (S = 0.650) is shown in Figure 11. Comparison with Figure 10 (where S = 0.130) shows that peak efficiency for the optimum spacing was somewhat better and the

efficiency was higher over a wider flow ratio range.

The second case was tested by constructing a special lucite throat-diffuser section identical in detail with the first lucite section, with the exception that the throat length was increased to 5.13 inches. Performance curves for this section are as shown in Figure 12. Mixing of the water and air took place prior to the diffuser entrance for the entire flow ratio range with the exception of the high back pressure portion just prior to "Cutoff" where air flow goes to zero. Here the flow pattern, as sketched in Figure 12, has an unsteady appearance similar to cavitation. This phenomenon occurs over the range of ϕ_d values that include the narrow peak on the efficiency curve, and may explain this sudden change in performance. In this area the back pressure has little effect on the flow ratio; e.g., an increase in the back pressure from 19 psig to 23 psig decreased the flow ratio from 0.0736 to 0.0556.

Comparison with Other Studies

In general, these data compare satisfactorily with performance data reported by Folsom (5). The water jet air pump used in Folsom's study had an area ratio, b, of 0.45 and the primary and secondary flow rates were larger because of the difference in the size of the equipment. Despite these differences the performance curves show the same trends. Peak efficiencies of about 16% were reported by Folsom. The maximum efficiency obtained in the present study was about 13% for an area ratio of $b = 0.4$.

Takashima (6) observed that as the diffuser section back pressure increased the solid jet stream into the diffuser section backed up until complete break-up was accomplished in the throat. In addition he

observed that nozzle-to-throat spacing had little effect on pump efficiency. As shown in Figure 10 the flow patterns observed in the present study tend to corroborate Takashima's findings. However, as shown in the previous section the nozzle-to-throat spacing does have an effect on pump efficiency.

CHAPTER IV

DESIGN PROCEDURE

Water jet air pump performance can be described by the water and air flow rates, and the nozzle side port, and discharge pressures. The pump itself is described by the nozzle and throat areas, a and A respectively. In addition the following dimensionless flow and pressure ratios are used ϕ_d, N and α which are defined in Appendix B.

Design Example:

A water jet air pump is to be designed knowing the discharge pressure and the air flow rate, with high flow ratio required.

Given: W_2, P_d

Find: W_1, P_n, b, s, a, A

Since ϕ_d at maximum efficiency decreases as b increases, the smallest area ratio used in this work, b = 0.2, will be selected in order to attain the desired "high flow ratio" characteristic.

Inspection of Figure 7 shows that high efficiency and the limit of agreement with the theoretical solution occurs at $\phi_d = 0.24$. With this value of ϕ_d where $N \ln \alpha = 0.37$, efficiency η is equal to $\phi_d N \ln \alpha = 8.9$ per cent. Nozzle flow rate Q_1 can be found from $\phi_d = \frac{Q_{2s}}{Q_1}$ from which W_1 can be calculated using $W_1 = \rho_1 Q_1$ (ρ_1 is a constant.) ϕ_s can be found using $\phi_s P_s = \phi_d P_d$. Values of K_1 and K_{34} can be assumed to be 0.1 and 0.3. Since P_s is usually near atmospheric the ratios of equations 13 and 15 will yield a value of N which in turn can be used to calculate P_n. Nozzle area, a, is found from:

$$\bar{P}_n - P_s = \frac{\rho_1 V_{1s}^2}{2g_c} [1 + K_1] \qquad (14)$$

and the continuity relation

$$W_1 = \rho_1 V_{1s} a$$

The throat area, A, is found from $b = \frac{a}{A}$.

Nozzle-to-throat spacing is found by referring to table I.

CHAPTER V

SUMMARY AND CONCLUSIONS

Statement of the Problem

The purpose of this investigation was to develop a theoretical analysis and compare this with experimental results, and to determine the effects of nozzle-to-throat section area ratio and nozzle tip to throat entrance spacing upon pump performance.

Procedure of the Investigation

The theoretical analysis developed in Chapter II was based on integration of the differential equation of motion, treating the density of the liquid-gas mixture as a variable. The theoretical treatment is based on the use of K_1 and K_{34} coefficients measured with liquid/liquid flow conditions.

The nozzle pressure was varied from 10 to 100 psig, the back pressure flow 0 to 71 psig, and the suction chamber pressure from 14.03 to 3.44 psia. The flow rate of water was varied from 43.3 to 71 lb_m/min, and that of air from 0 to 1.075 cu. ft./min.

Results

A function of the dimensionless pressure ratios N and L was plotted as a function of the flow ratio ϕ_d, as shown in Figures 7 through 10. Numerical results are listed in the test data section, Appendix C. The actual pump performance coincides with the theory, shown as a solid line in Figures 7 through 10, up to a certain point and then falls away rapidly. The point at which this rapid decline occurs coincides with the point at which mixing no longer occurs in the throat, as shown in the accompanying sketches of the mixing patterns. Since the mixing

occurs in the diffuser and the mixing loss is directly proportional to the area, the mixing loss increases rapidly causing a sharp decline in efficiency.

Conclusions

(1) The performance of the water jet air pump can be satisfactorily predicted by the equations developed in Chapter II.

(2) Comparison of theory and experiment plus observation using the specially constructed transparent throat-diffuser section has shown:

   (a) Flow ratio ϕ_d for maximum efficiency decreases with increasing area ratio b as predicted by theory.

   (b) Maximum efficiency is obtained when jet break-up occurs in the throat. Hence the pump should be designed and operated to maintain this break-up in the throat.

(3) At an area ratio b = 0.6, using an unusually long throat, an unsteady "front" resembling cavitation occurred in the throat. Under these conditions pump performance agreed well with theoretical predictions. When the "cavitation" zone moved out into the diffuser entrance, actual efficiency decreased rapidly below the predicted value.

(4) Although it is possible to calculate P_t, direct measurement would be highly desirable in any future work. This measurement would permit direct calculation of friction coefficients from experimental data.

BIBLIOGRAPHY

1. "A Simple Air Ejector," Keenan, J. H. and Neumann, E. P. Journal of Applied Mechanics, vol. 69, 1942.

2. "The Water Jet Pump," Gosline, J. E. and O'Brien, M. P., University of California Publications in Engineering, vol. 3, no. 3, 1934, pp. 167-190.

3. "The Design of Jet Pumps," Flugel, G. NACA T.M., 982, 1939.

4. von Pawel-Rammingen, G. Doctors' Dissertation, Braunschweig, 1936.

5. "Jet Pumps with Liquid Drive," Folsom, R. G., Chemical Engineering Progress, vol. 44, no. 10, 1948, pp. 765-770.

6. "Studies on Liquid-Jet Gas Pumps," Takashima, Y. Journal of the Scientific Research Institute, (Tokyo), vol. 46, 1952, pp. 230-246.

7. "Jet Pump Theory and Performance with Fluids of High Viscosity," Cunningham, R. G., American Society of Mechanical Engineers Transactions, Nov. 1957.

8. "Design of Injectors for Low Pressure Air Flow," McElroy, G. E., Bureau of Mines Technical Paper, G78, 1945.

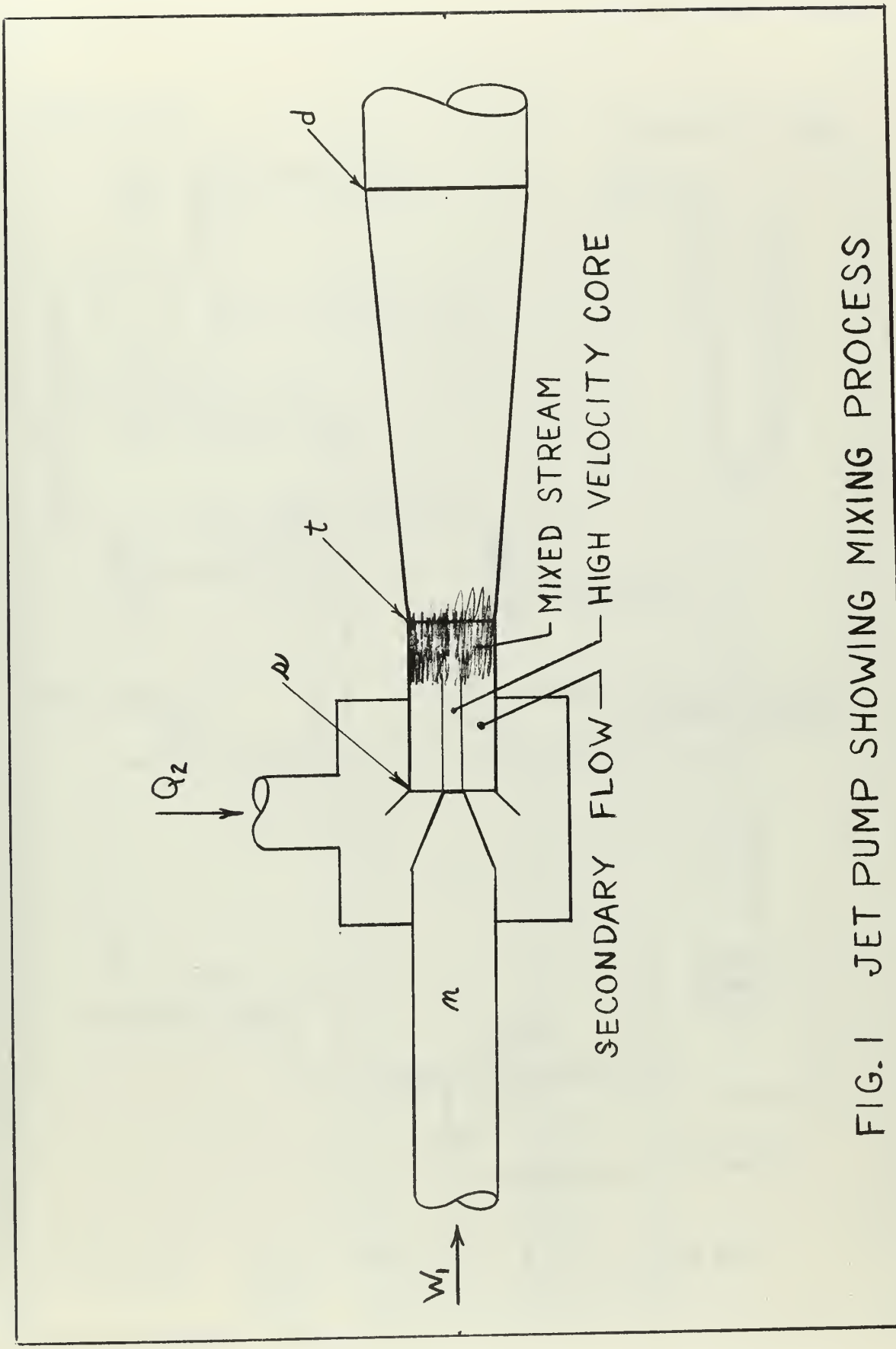

FIG. 1 JET PUMP SHOWING MIXING PROCESS

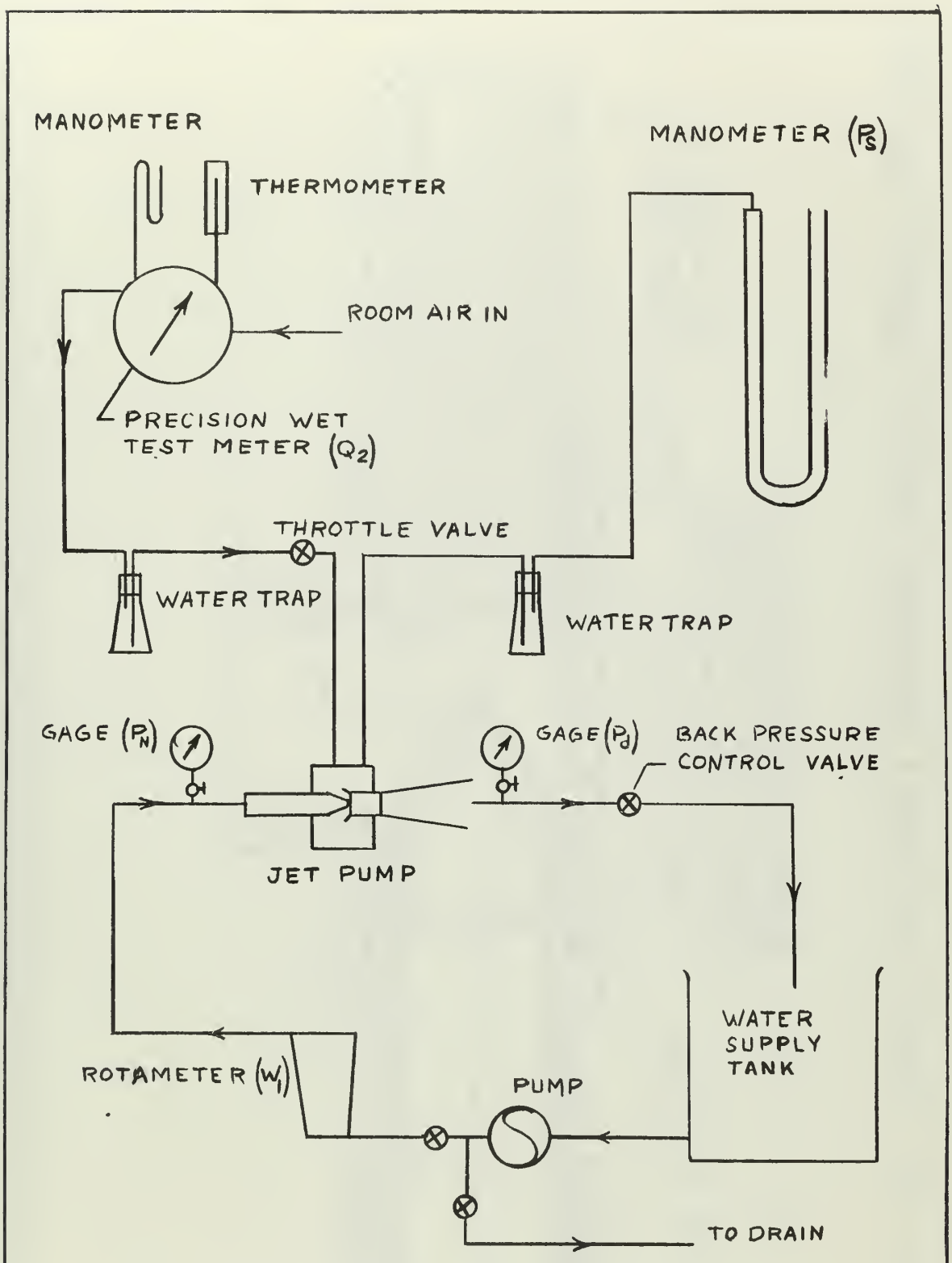

FIG. 2 JET PUMP TEST STAND AND FLOW DIAGRAM

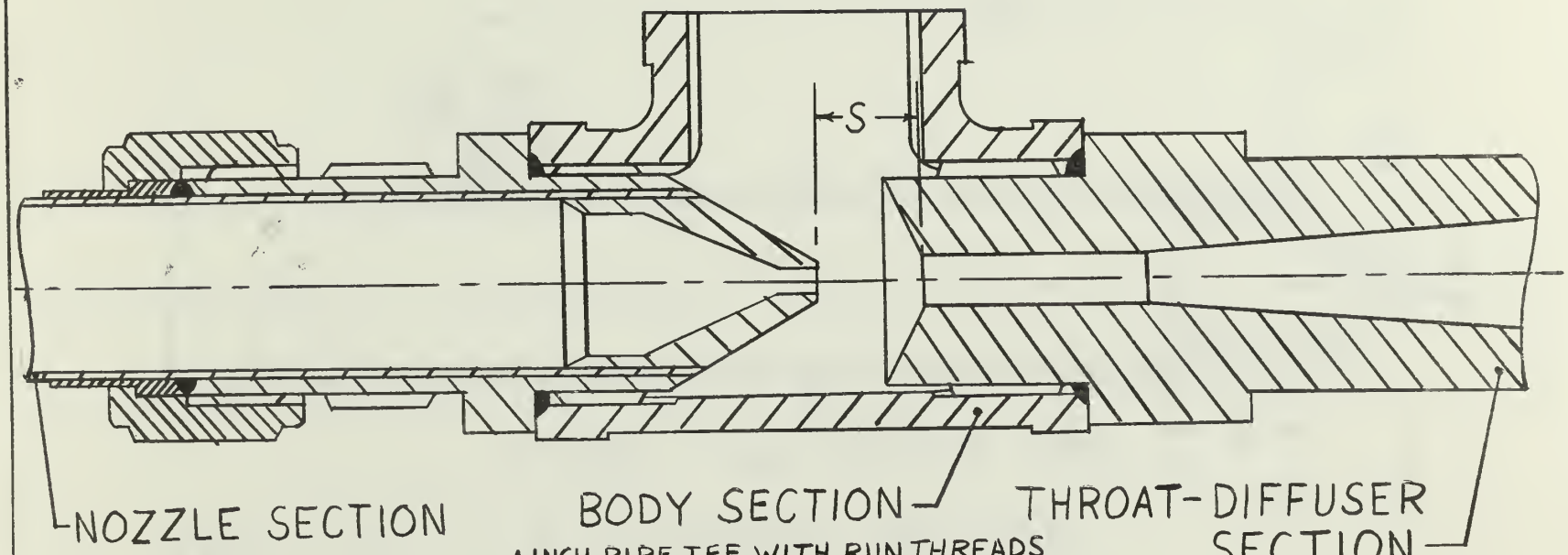

FIG. 3 JET PUMP ASSEMBLY SHOWING NOZZLE-THROAT SPACING, S

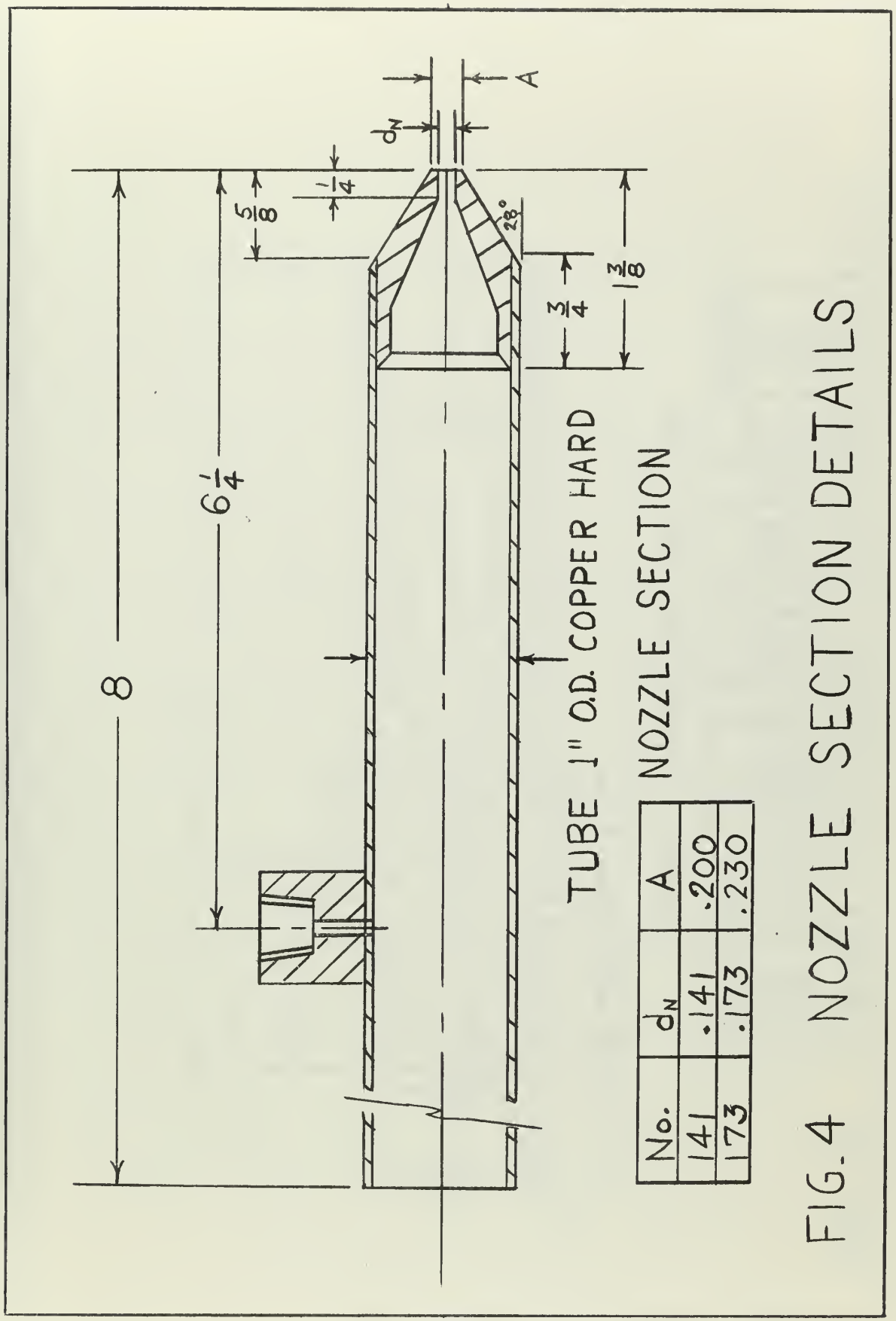

No.	d_N	A
141	.141	.200
173	.173	.230

FIG. 4 NOZZLE SECTION DETAILS

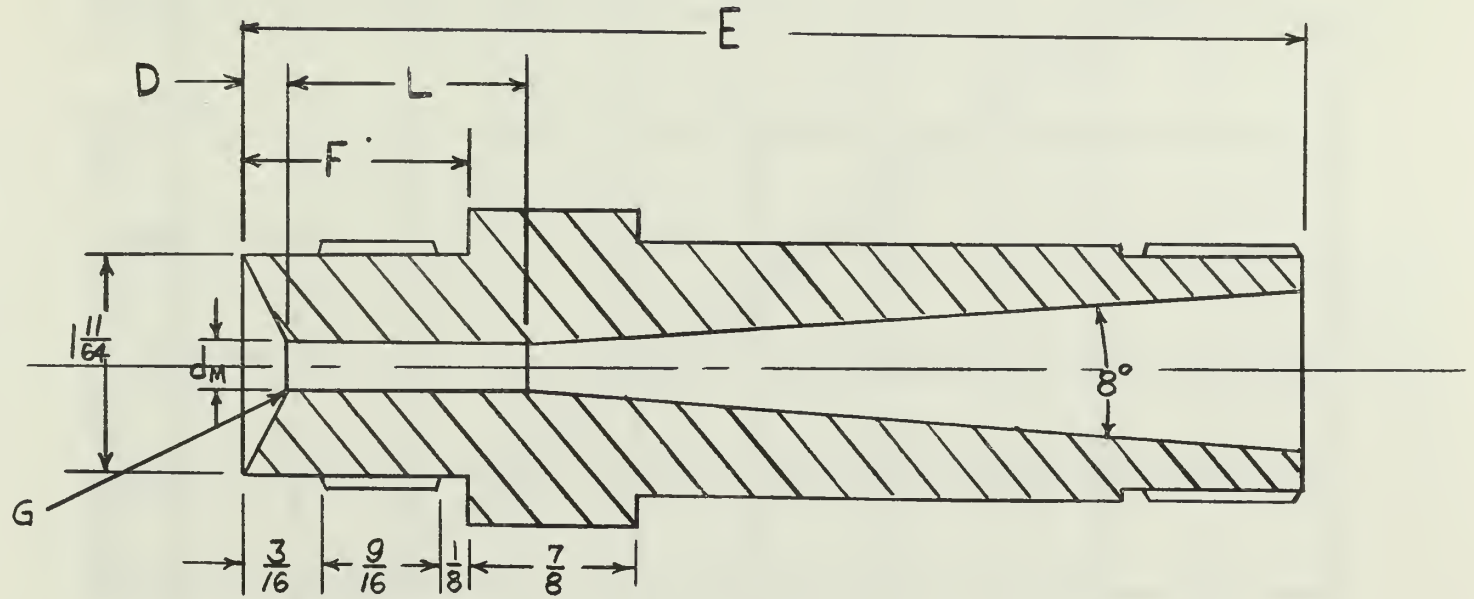

THROAT-DIFFUSER SECTION

No.	d_M	L	D	E	F	G-RADIUS
224	.224	.896	.263	5.768	.937	1/8
316	.316	1.264	.218	5.477	.875	1/8

FIG. 5 THROAT-DIFFUSER SECTION DETAILS

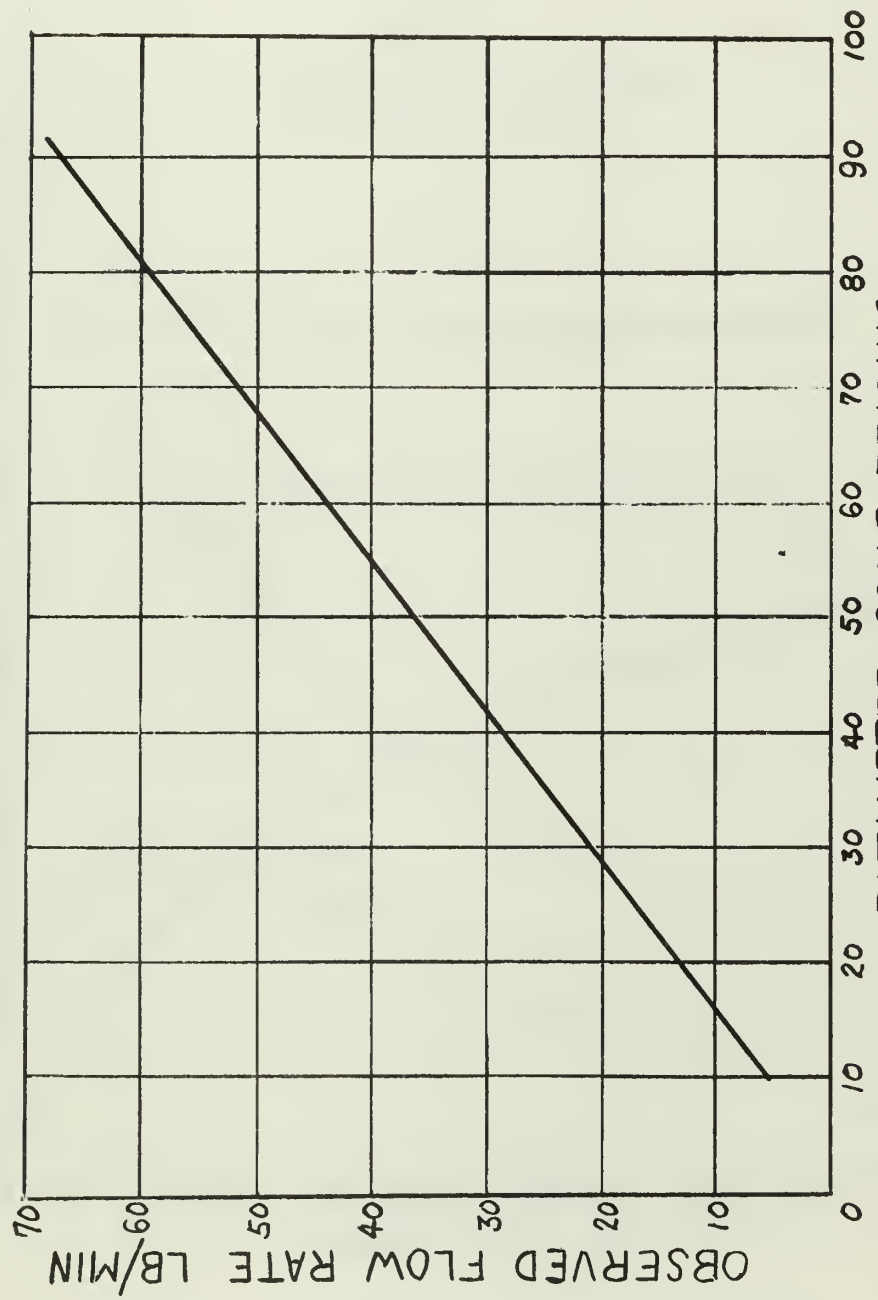

FIG. 6 ROTAMETER CALIBRATION

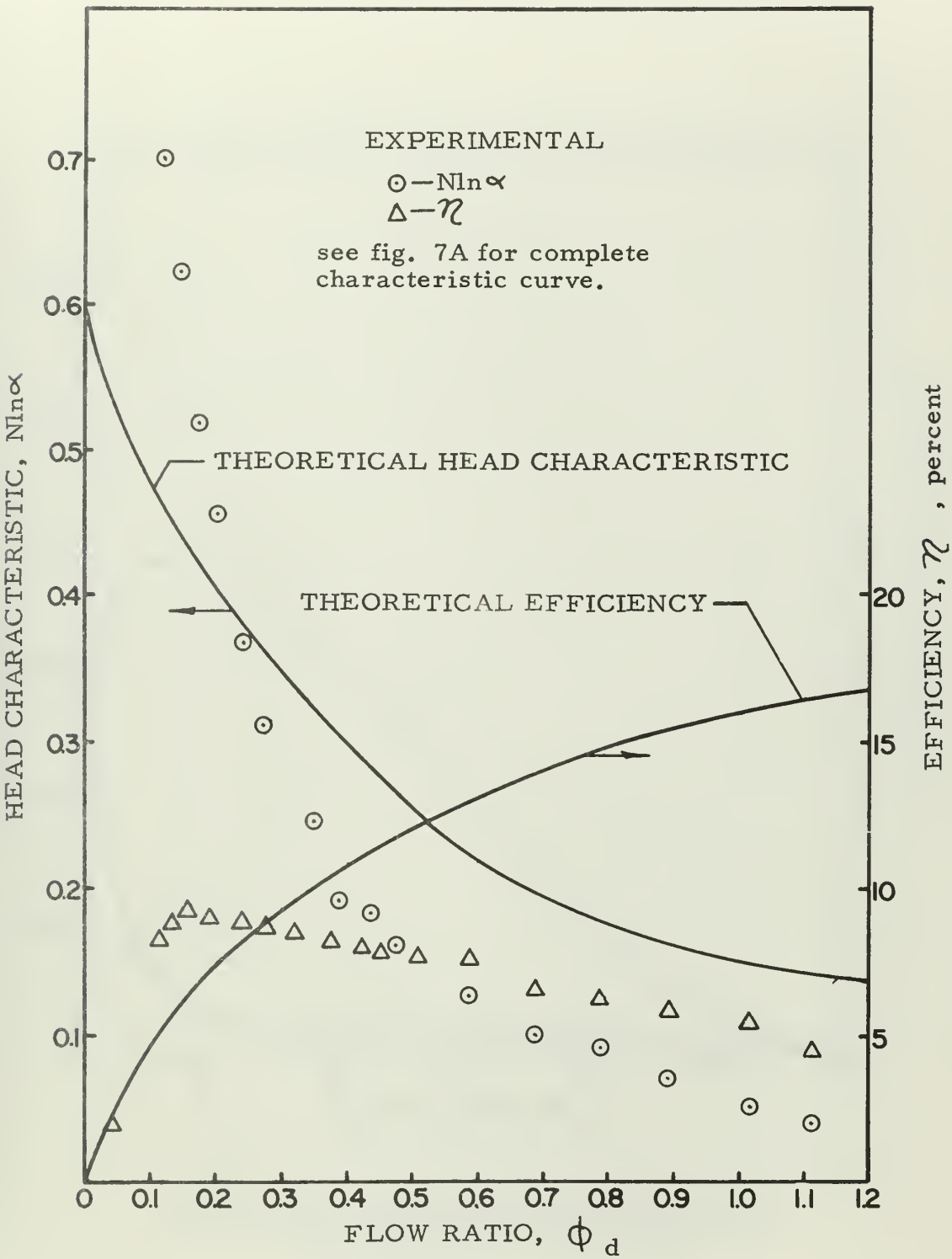

Fig. 7 Head Characteristic and Efficiency vs Flow Ratio, b = 0.2.

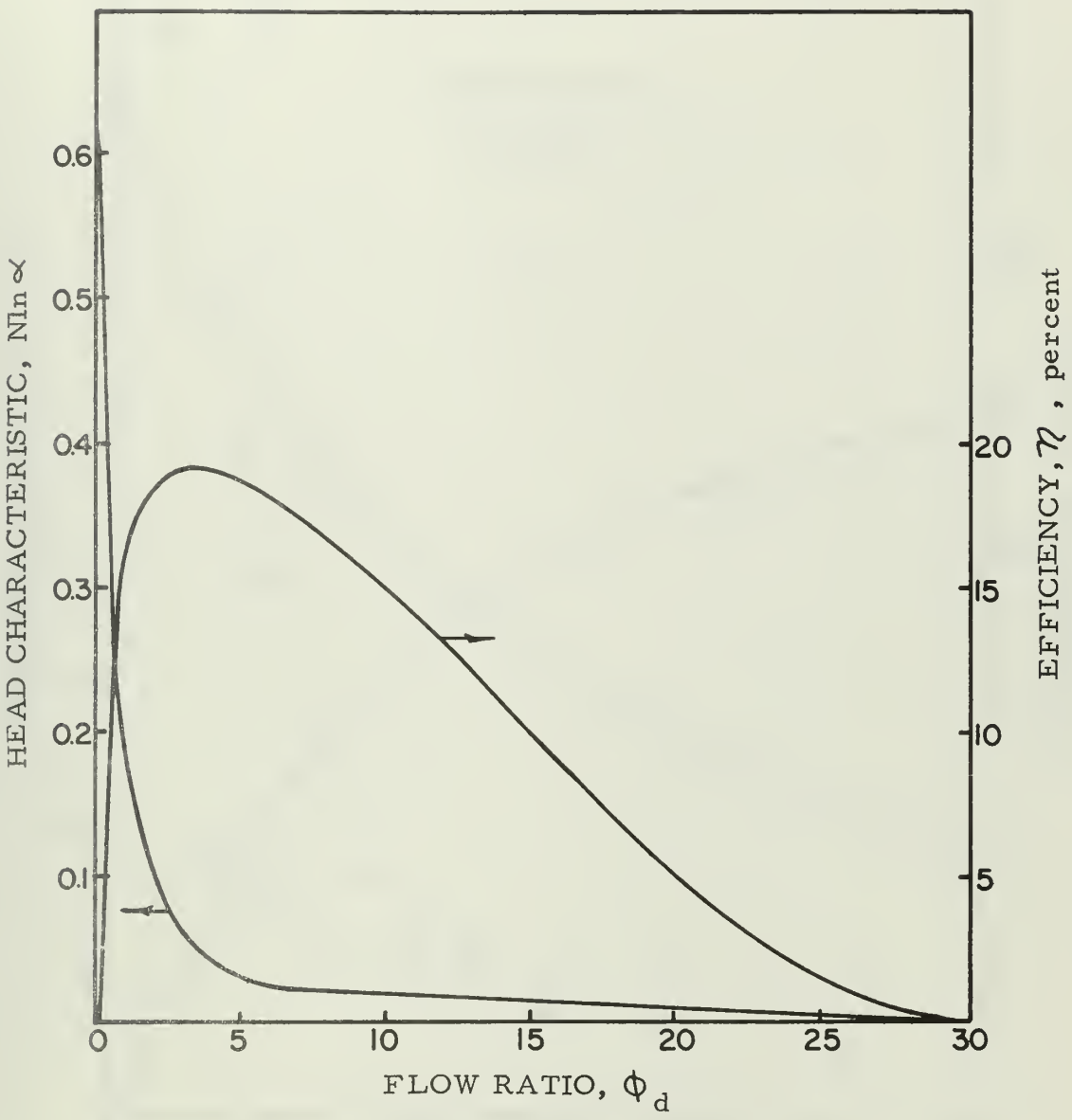

Fig. 7A Head Characteristic and Efficiency vs Flow Ratio, b = 0.2.

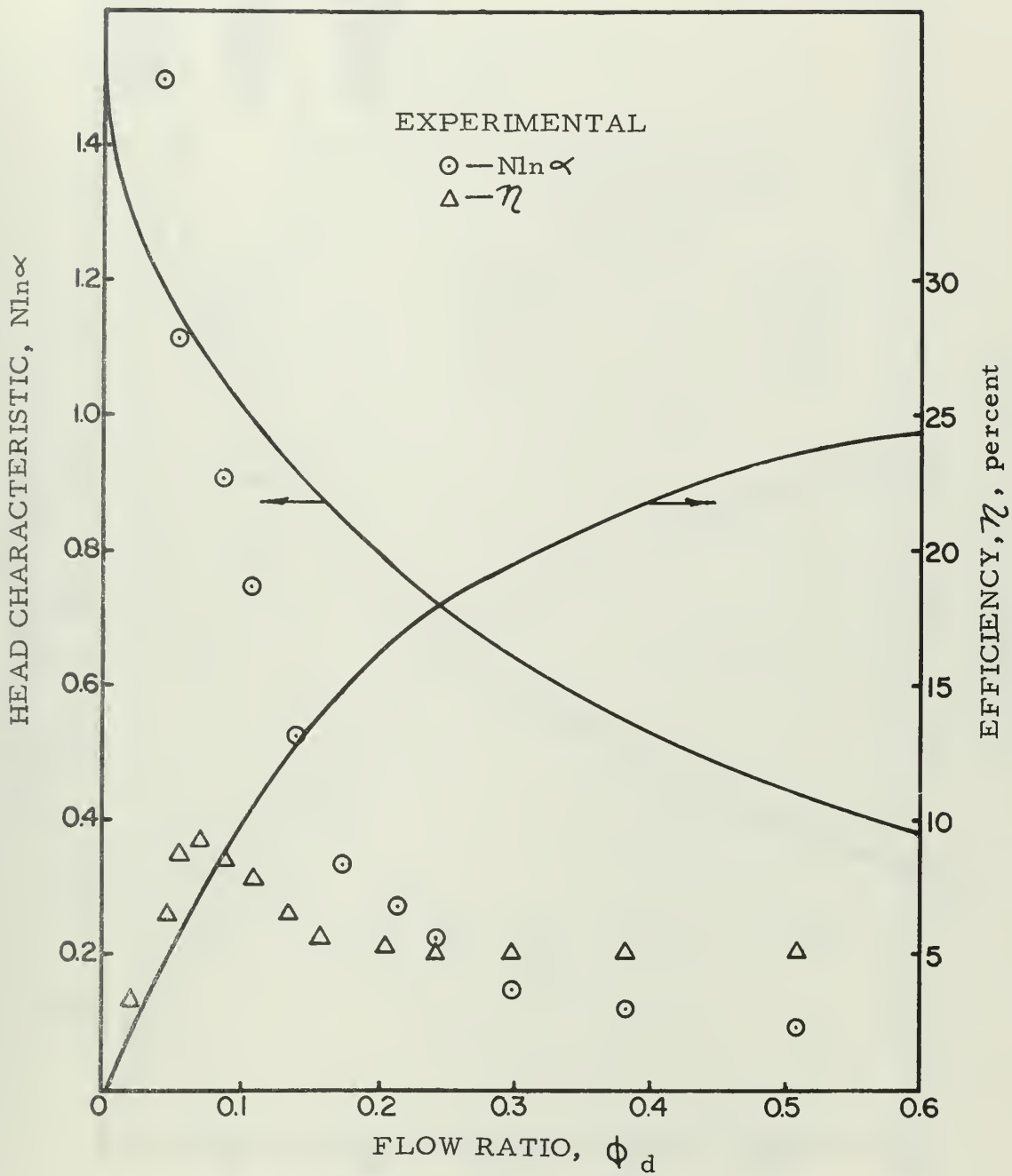

Fig. 8 Head Characteristic and Efficiency vs Flow Ratio, b = 0.3.

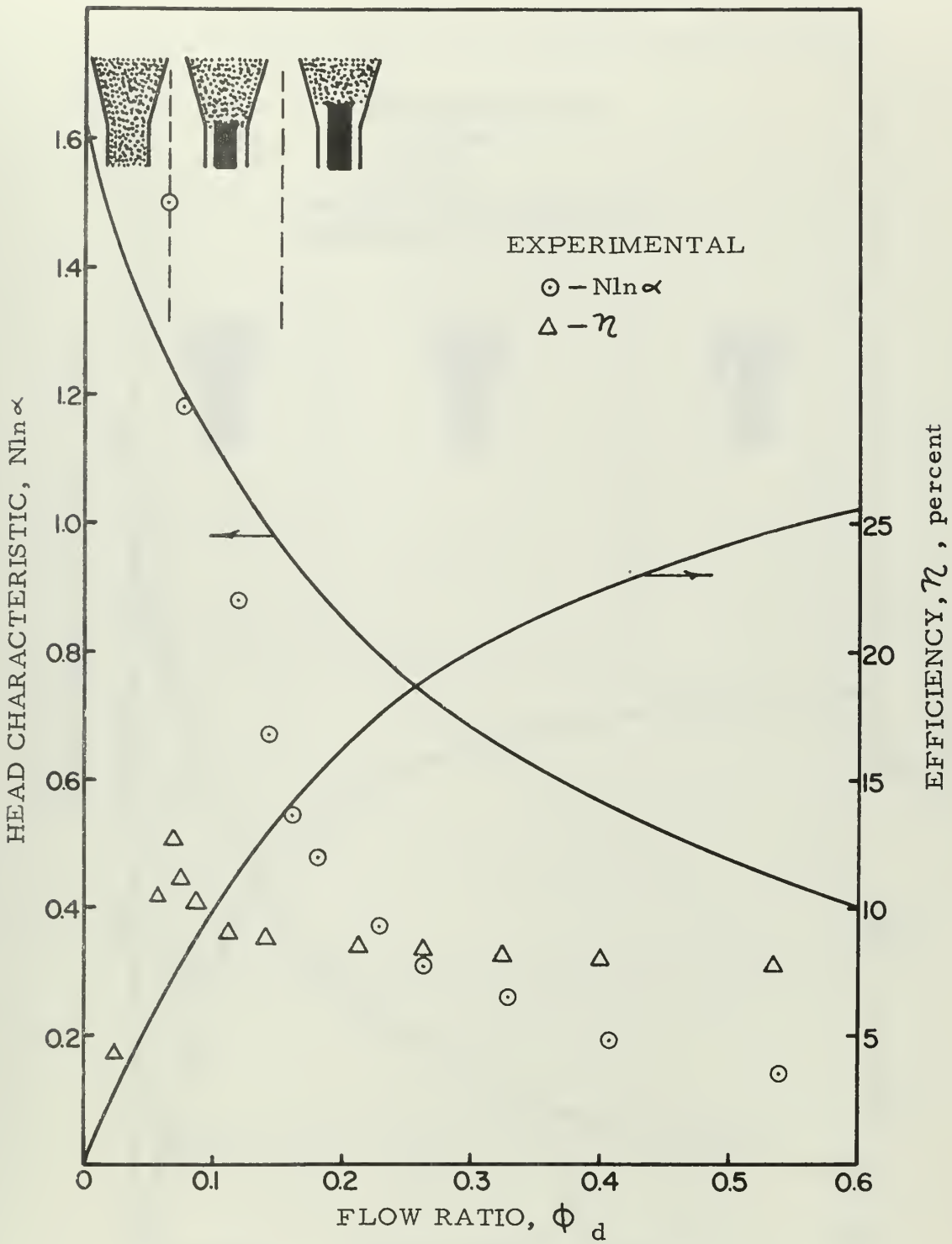

Fig. 9 Head Characteristic and Efficiency vs Flow Ratio, b = 0.4.

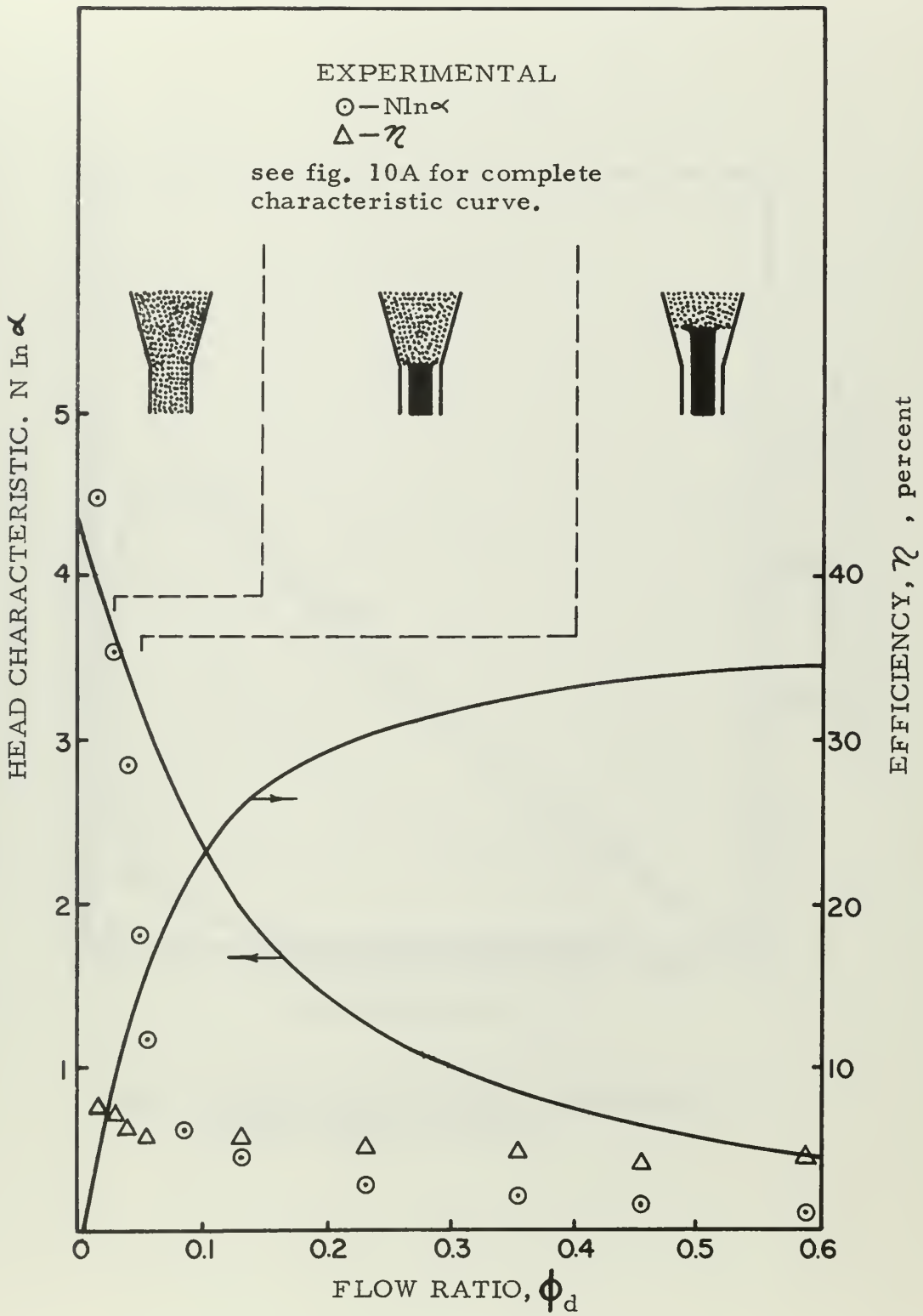

Fig. 10. Head Characteristic and Efficiency vs Flow Ratio, b = 0.6.

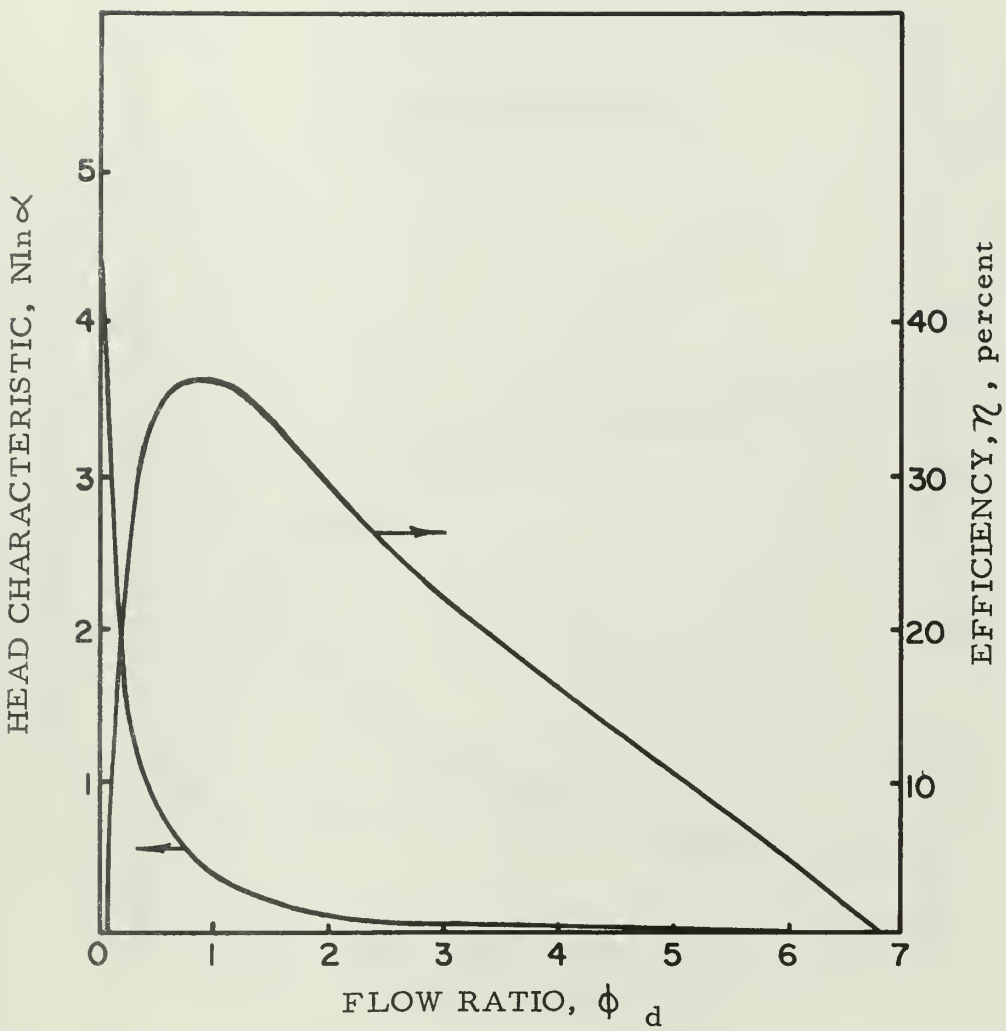

Fig. 10A Head Characteristic and Efficiency vs Flow Ratio, b = 0.6.

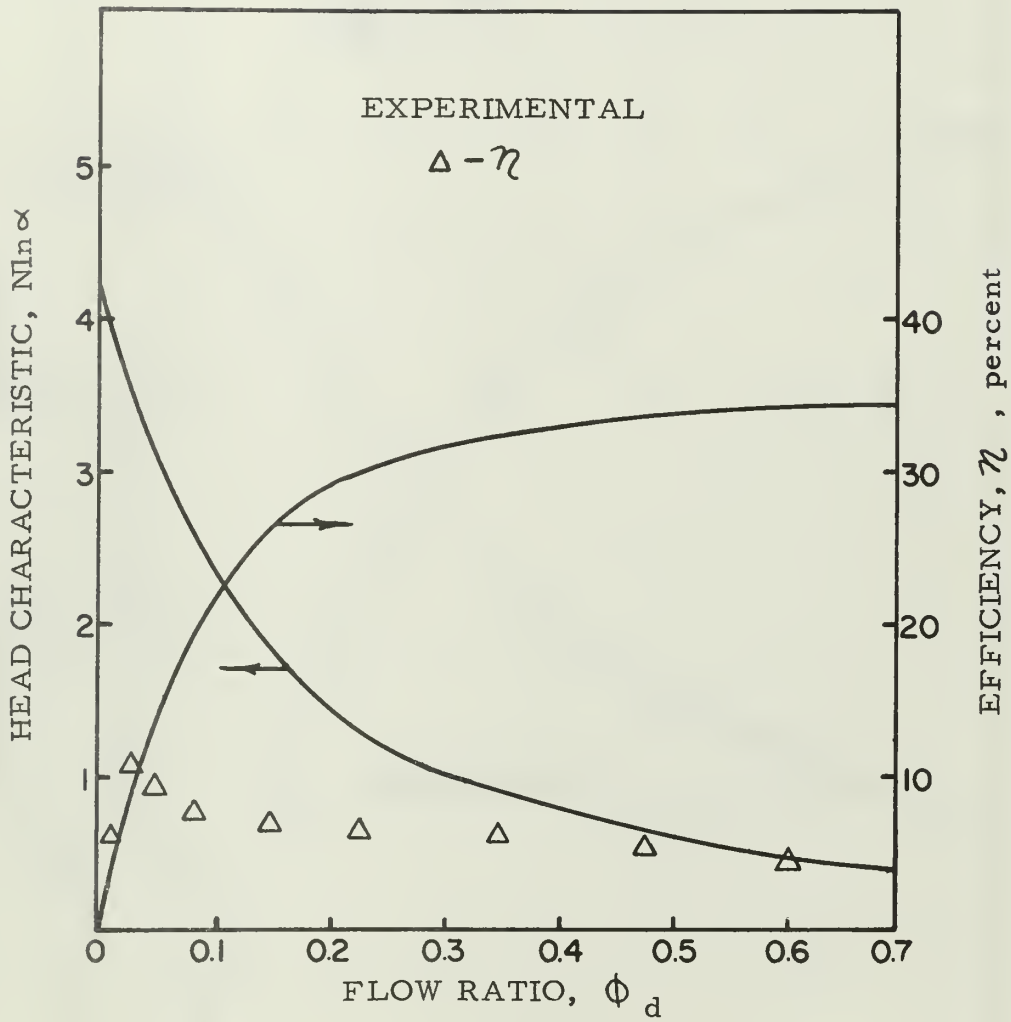

Fig. 11 Head Characteristic and Efficiency vs Flow Ratio, b = 0.6. (For pump at optimum spacing.)

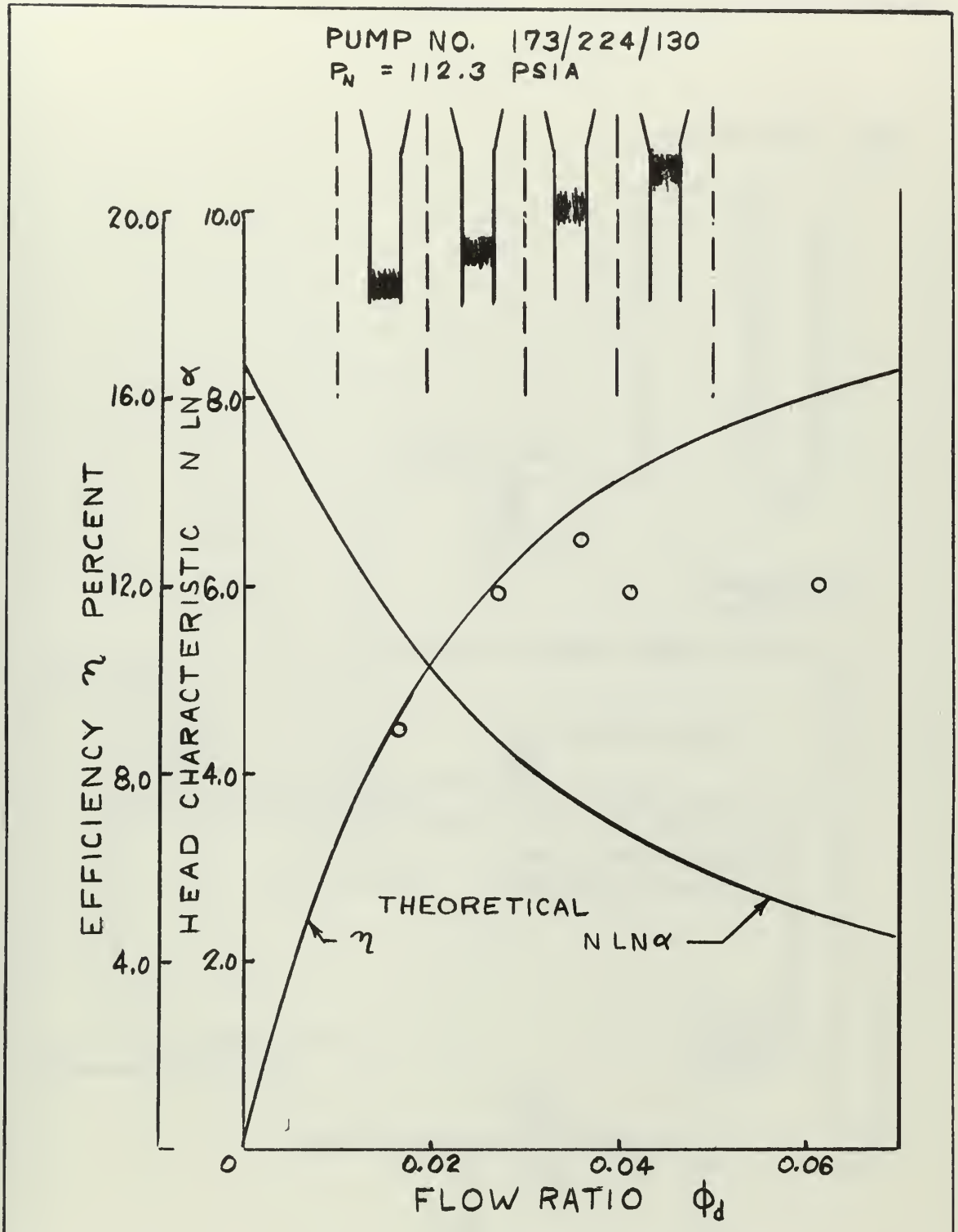

FIG. 12 HEAD CHARACTERISTIC AND EFFICIENCY VS. FLOW RATIO b=0.6 FOR LUCITE SECTION HAVING THROAT LENGTH L = 5.312 INCHES

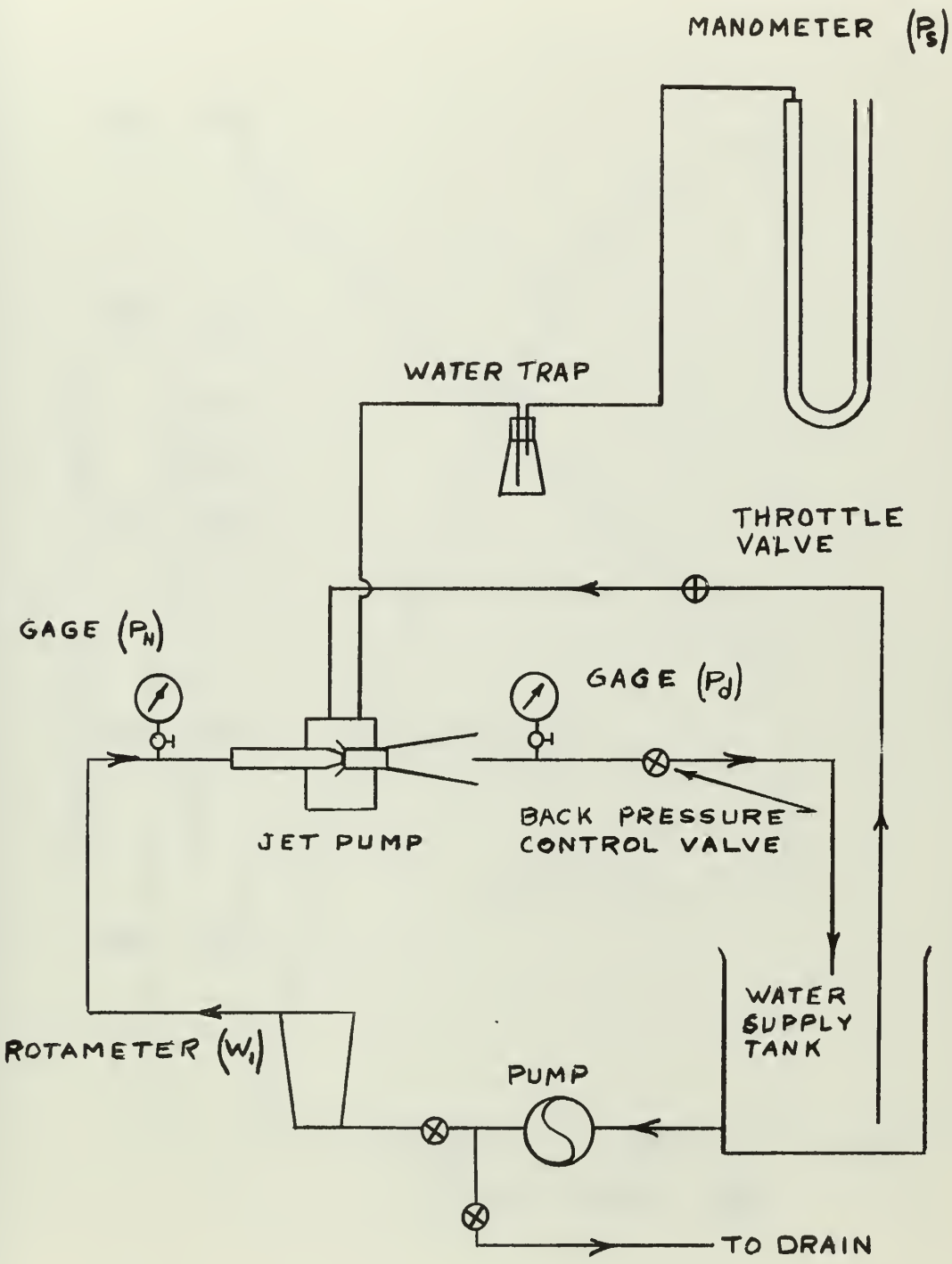

FIG. 13 JET PUMP TEST STAND SHOWING MODIFICATION FOR USE AS WATER JET PUMP

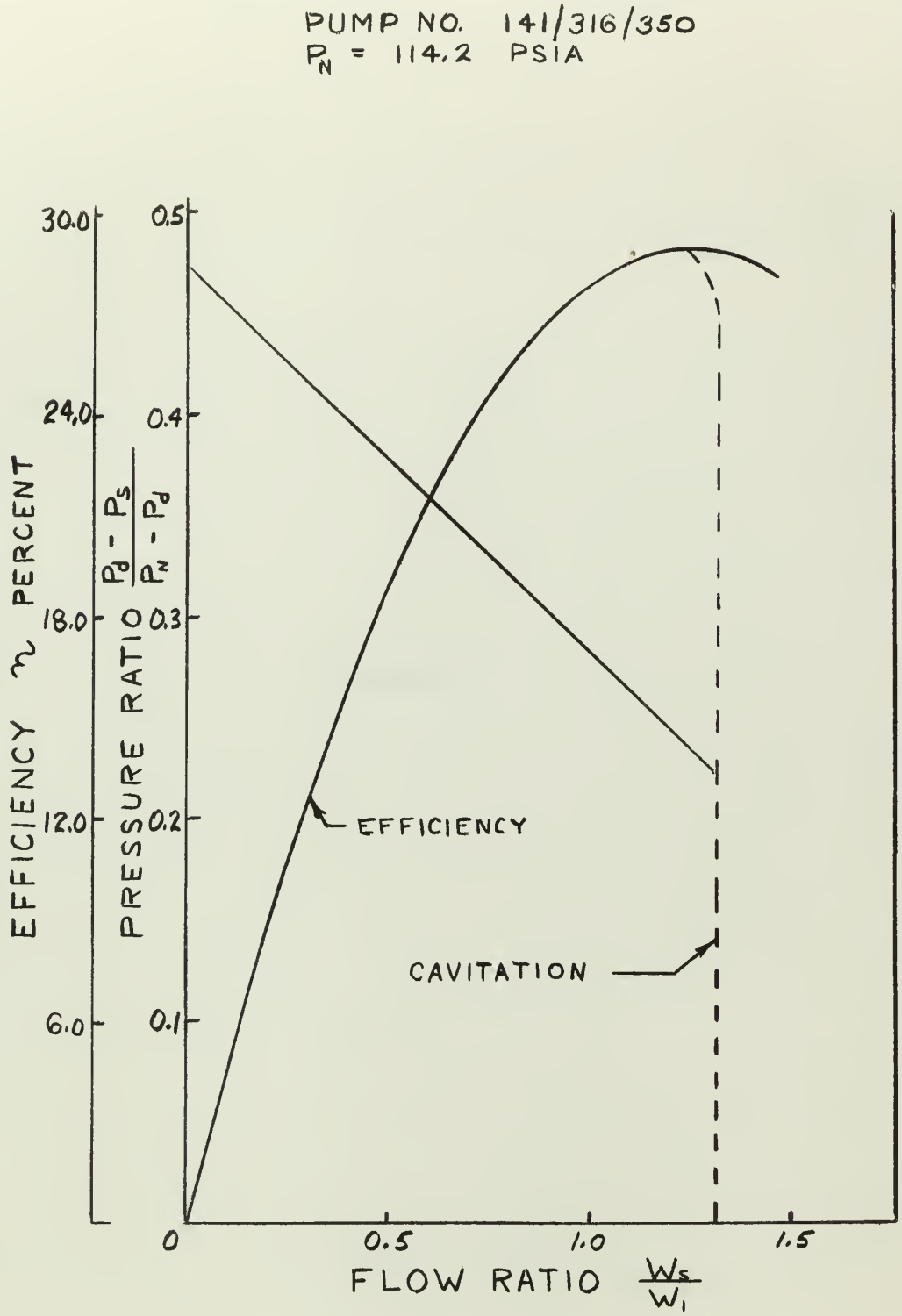

FIG. 14 EXPERIMENTAL PRESSURE RATIO AND EFFICIENCY VS FLOW RATIO FOR WATER JET PUMP

APPENDIX A

Apparatus Used as Water Jet Pump:

Comparison with Other Studies

As described in Chapter III the experimental apparatus was modified to act as a water jet pump in order to measure experimentally the friction coefficients K_1, K_{34} and to permit a comparison with prior studies. See Figure 13.

The tests were conducted by holding constant the primary flow rate and the suction chamber pressure while the back pressure was varied from the "cutoff" pressure (where the secondary mass flow rate equals zero) to the pressure producing the maximum flow obtainable, ie: where the back pressure valve was wide open. At each point nozzle pressure, suction chamber pressure, diffuser discharge pressure, primary mass flow rate and secondary mass flow rate were recorded.

The ratio of secondary to primary mass flow rates was then plotted as a function of the ratio of the back pressure-suction chamber pressure difference to nozzle pressure-back pressure difference as shown in Figure 14 for jet pump 141/316/350. Similar results were obtained for other area ratios and will not be shown. Numerical results are listed in the test data section, Appendix C.

The approximate theoretical approach used by Cunningham (7) was used to calculate values for the nozzle and throat-diffuser constants K_1 and K_{34} respectively. With $K_1 = .18$ and $K_{34} = .051$ calculated from the experimental data a satisfactory comparison was made with Figure 14 (7), that is maximum flow ratio ϕ_o and zero flow ratio N_o were calculated for the area ratio used ($b = 0.2$), and found to be $N_o = .477$ and $\phi_o = 2.6$. These compare with $N_o = .47$ and $\phi_o = 2.5$ taken from Figure 14 (7).

APPENDIX B

Sample Calculations

The tests were conducted by operating the pump at a fixed primary flow W_1 and fixed suction port pressure P_s. The discharge pressure P_d was then varied from zero where the air flow rate was a maximum to the "cutoff" pressure where the air flow rate went to zero. The water and air flow rates, and the three pressures P_n, P_s, and P_d were recorded for each run. These data were then used to calculate the pressure ratios N and α and the flow ratio ϕ_d as shown below. The water flow rate was set by rotameter and then measured by weighing against a stop watch. The air flow rate was measured by a precision wet test meter.

Test Date: 4/13/62

Pump Number: 173/224/120, b = 0.6

Barometer: 28.57 in Hg corrected

Air Temperature: 83.5°F

Water Temperature: 53°F

$Q_2 = 0.121 \quad ft^3/min \quad$ (at 14.02 psia)

$W_1 = 71\ lb_m/min$

$P_n = 99.0$ psig corrected for gage calibration error

$P_s = -5.8$ in Hg or 11.18 psia

$P_d = 60.0$ psig corrected for gage calibration error

$$\alpha = \frac{P_d}{P_s} = \frac{74.03}{11.18} = 6.64$$

$$N = \frac{P_d}{P_n - P_d} = \frac{74.03}{99.0 - 60.0} = 1.9$$

$N \ln \alpha = 3.6$

$$\phi_d = \frac{W_2 \rho_1}{W_1 \rho_{2d}} = 12.22 \qquad \frac{Q_2}{P_d} = 0.02$$

$$\phi_s = \frac{\phi_d P_d}{P_s} = 0.02 \quad \frac{(74.03)}{(11.18)} = 0.132$$

The calculated $N \ln \alpha$ values were then plotted against flow ratio ϕ_d, and a smooth curve faired through the points. An efficiency curve $\eta = \phi_d N \ln \alpha$ was plotted by multiplying $N \ln \alpha$ values from the curve by the corresponding value of ϕ_d.

APPENDIX C

Date 4/10/62 Barometer 28.97 in Hg.

Rotameter 59 Reference: Figure 7 14.23 psia

b 0.2 141/316/308 T_1 54°F

T_2 78°F

P_n psig	P_s in. Hg	P_d psig	W lbm/min	Q_2 cuft/min	N	$\frac{\alpha}{\ln \alpha}$	$N_{\ln \alpha}$	ϕ_d	η %
	-4.8	0	43.3	.950	.1423	1.20 / .182	.0259	1.345	3.48
		1		.035	.1540	1.282 / .248	.0382	1.105	4.22
		2		.835	.1659	1.370 / .315	.0523	1.036	5.41
		3		.760	.1779	1.451 / .372	.0662	.887	5.88
		4		.700	.1900	1.535 / .429	.0815	.774	6.30
		5		.640	.2025	1.621 / .483	.0979	.671	6.57
		6		.580	.2150	1.710 / .536	.1152	.577	6.6
		7		.547	.2285	1.790 / .582	.1330	.518	6.9
		8		.500	.2415	1.875 / .628	.1515	.452	6.87
		9		.480	.2555	1.960 / .673	.1720	.416	7.15
		10		.458	.2690	2.045 / .715	.1924	.379	7.3
		12		.420	.2980	2.210 / .793	.2360	.323	7.61
		15		.380	.3440	2.465 / .902	.3100	.261	8.1
		17		.360	.3760	2.630 / .966	.3630	.232	8.42
		20		.336	.4280	2.890 / 1.06	.4540	.1975	8.96
		22		.313	.4650	3.055 / 1.117	.520	.174	9.05
		25		.272	.5240	3.310 / 1.196	.626	.1415	8.86
		27		.232	.5650	3.470 / 1.245	.704	.1135	7.99
		30		.087	.6310	3.730 / 1.318	.832	.0405	3.37

Date 4/13/62 Barometer 28.50 in Hg.

Rotameter 93 Reference: Figure 8 14.00 psia

b 0.3 T_1 53°F

173/316/237 T_2 82°F

P_n psig	P_s in. Hg.	P_d psig	$W_1 \frac{lbm}{min}$	$Q_2 \frac{cuft}{min}$	N	$\frac{\alpha}{\ln \alpha}$	N ln α	ϕ_d	$\eta_{\%/100}$
				1.075		1.302			
98.5	-6.6	0	71	1.075	.142	.264	.0375	.941	.0353
				.883		1.488			
		2		.882	.1658	.398	.066	.676	.0446
				.754		1.673			
		4		.755	.1905	.515	.0982	.514	.0504
				.620		1.858			
		6		.628	.216	.619	.134	.382	.0512
				.54		2.045			
		8		.54	.243	.715	.174	.300	.0522
						2.23			
		10		.48	.271	.802	.217	.245	.0532
						2.41			
		12		.450	.301	880	.265	.21	.0557
						2.69			
		15		.377	.347	.989	.343	.1592	.0546
						3.16			
		20		.355	.433	1.15	.498	.128	.0638
						3.62			
		25		.336	.531	1.285	.682	.1056	.072
						4.09			
		30		.319	.642	1.41	.908	.0889	.0805
						4.56			
		35		.290	.772	1.52	1.171	.0725	.085
						5.01			
		40		.247	.924	1.61	1.485	.056	.0832
						5.30			
		43		.185	1.025	1.67	1.712	.0398	.0681
						5.48			
		45		.084	1.104	1.70	1.88	.01745	.0328
						5.62			
		46.5		0	1.162	1.725	2.005	0	0

Date 4/12/62 Barometer 29.02 in Hg. 14.25 psia

Rotameter 50 Reference: Figure 9 T_1 54°F

b 0.4 141/224/291 T_2 84°F

P_n psig	P_s in Hg.	P_d psig	W_1 $\frac{lbm}{min}$	Q_2 $\frac{cuft}{min}$	N	$\frac{\alpha}{\ln \alpha}$	N ln α	ϕ_d	η %
				.903		1.104			
70	-2.7	0	36.6	.905	.2035	.099	.02015	1.51	.0304
				.680		1.258			
		2		.680	.239	.2295	.0548	.997	.0547
				.565		1.41			
		4		.565	.276	.3435	.0947	.737	.0698
				.454		1.566			
		6		.455	.316	.449	.142	.534	.0757
				.382		1.721			
		8		.382	.359	.543	.1952	.408	.0798
						1.877			
		10		.330	.404	.629	.254	.324	.0824
						2.03			
		12		.290	.453	.708	.321	.263	.0845
						2.185			
		14		.258	.504	.781	.393	.2175	.0855
						2.34			
		16		.220	.56	.869	.487	.173	.0843
						2.495			
		18		.205	.621	.914	.568	.1514	.0875
						2.65			
		20		.191	.685	.975	.668	.1325	.0885
						2.96			
		24		.163	.788	1.085	.856	.1015	.0870
						3.27			
		28		.152	1.005	1.185	1.192	.0857	.1022
						3.58			
		32		.142	1.217	1.275	1.55	.073	.1133
						3.89			
		36		.137	1.475	1.359	2.0	.0649	.129
						4.04			
		38		.105	1.635	1.396	2.28	.0479	.1094
						4.2			
		40		.041	1.81	1.435	2.6	.0180	.0467
						4.275			
		41		0	1.905	1.452	2.77	0	0

4/13/62 Barometer 28.57 in Hg.

Rotameter 93.0 Reference: Figure 10 14.03 psia

b 0.6 173/224/120 T_1 53°F

T_2 83.5°F

P_n psig	P_s in Hg	P_d psig	W_1 lbm/min	Q_2 cuft/min	N	$\frac{\alpha}{\ln \alpha}$	N ln α	ϕ_d	$\eta_{\%/100}$
99	-5.8	0	71	1.055	.1418	1.255 / .227	.0322	.92	.0296
		2		.988	.1652	1.435 / .361	.0596	.751	.0448
		4		.875	.1896	1.613 / .478	.0905	.593	.0537
		6		.748	.2155	1.79 / .582	.1255	.455	.057
		8		.655	.242	1.98 / .683	.165	362	0597
		12		.485	.299	2.33 / .845	.252	.2275	.0573
		15		.415	.346	2.6 / .955	.331	.1745	.0577
		20		.330	.431	3.04 / 1.112	.480	.1185	.057
		25		.279	.528	3.49 / 1.25	.66	.0874	.0577
		30		231	.638	3.94 / 1.37	.875	.0641	0561
		35		.195	.767	4.39 / 1.48	1.135	.0486	.0551
		40		.167	.916	4.83 / 1.575	1.441	.0377	.0544
		45		.150	1.093	5.28 / 1.665	1.82	.0311	.0566
		50		.136	1.307	5.73 / 1.745	2.28	.02595	0592
		55		.129	1.57	6.19 / 1.82	2.855	.0228	.0651
		60		.121	1.9	6.64 / 1.892	3.6	.01998	.0719
		65		.112	2.32	7.08 / 1.956	4.54	.0173	0785
		70		.108	2.9	7.52 / 2.02	5.86	.0157	.092
		71		.0	3.03	7.61 / 2.03	6.15	0	0